

# On the $\alpha$ -relaxation in bulk polyoxymethylene

R. W. GRAY\*

Department of Engineering Science, Oxford University, Parks Road, Oxford, UK

Values quoted for  $\Delta H_\alpha$ , the activation energy of the high temperature  $\alpha$ -relaxation in polyoxymethylene (POM), range from 20 to 92 kcal mol<sup>-1</sup>. This paper seeks to rationalize the discrepancy by remeasuring  $\Delta H_\alpha$  using time-temperature superposition of torsional creep and dynamic compliances for a POM specimen annealed at 160°C. Superposition of loss compliance curves  $J''(\omega, T)$  is possible over the range 20 to 120°C but creep compliance curves  $J(t, T)$  fail to superpose above about 70°C. The creep anomaly is explained in terms of the McCrum-Morris reduction equations in which the unrelaxed compliance  $J_U^T$  increases with temperature more rapidly than the relaxed compliance  $J_R^T$ . The activation energy  $\Delta H_\alpha$  has a constant value of  $21 \pm 1$  kcal mol<sup>-1</sup> below about 70°C. Above about 70°C,  $\Delta H_\alpha$  increases steadily up to  $33 \pm 2$  kcal mol<sup>-1</sup> at 120°C.

## 1. Introduction

Polyoxymethylene (POM) is a crystalline polymer with a melting point of about 185°C. The relaxation behaviour of this polymer has been extensively studied and has been reviewed by McCrum *et al* [1]. There are three familiar loss peaks termed  $\alpha$ ,  $\beta$  and  $\gamma$  which appear at 1 Hz at about 135, -10 and -70°C, respectively. Recently, two more relaxations have been reported [2], one at about -225°C ( $\delta$ ) and the other below -259°C ( $\epsilon$ ). In this paper only the high temperature  $\alpha$ -relaxation will be under discussion.

The  $\alpha$ -relaxation in POM has been studied by many authors [3-12] using both mechanical and dielectrical techniques over various ranges of temperature and frequency. It is generally accepted [5, 7-12] that the  $\alpha$ -relaxation (in common with many other crystalline polymers) involves large-scale chain motion in the crystalline regions of the polymer, although the precise mechanism remains unclear. Further, there is still a large and unexplained discrepancy between the published values for the activation energy  $\Delta H_\alpha$ . Both Ishida *et al* [4] and Arisawa *et al* [8] using low frequency dielectric data obtained a value of 20 kcal mol<sup>-1</sup> for  $\Delta H_\alpha$ . On the other hand, Read and Williams [6] used low frequency mechanical measurements and found  $\Delta H_\alpha$  in the range 65 to 92 kcal mol<sup>-1</sup>. The high frequency

data of Thurn [3] also yields very high values for  $\Delta H_\alpha$  but the elastic after-effect method of McCrum [5] gives 24 kcal mol<sup>-1</sup>. Further dielectric measurements by Arisawa *et al* [9] led to a value of 33 kcal mol<sup>-1</sup>. In single crystals of POM, Takayanagi [10] reported a figure of 55 kcal mol<sup>-1</sup>. Finally, Miki *et al* [12] used superposition of forced oscillation data and proposed that the  $\alpha$ -relaxation has three components with activation energies of about 60 kcal mol<sup>-1</sup> below 40°C, 25 kcal mol<sup>-1</sup> below 95°C and 32 kcal mol<sup>-1</sup> above 95°C. It is clear that this wide range of activation energies is in need of some rationalization.

The purpose of this paper is to describe some high temperature creep experiments in POM, to recalculate the activation energy and to explain why  $\Delta H_\alpha$  values quoted in the literature are so disparate. Studying the  $\alpha$ -relaxation in creep enables more of the relaxation to be observed, unfettered by the melting process, than is possible by torsion pendulum or forced oscillation measurements. (The loss tangent or the  $\alpha$ -relaxation has its maximum at 1 Hz at about 135°C and above 160°C the crystallinity starts falling rapidly.) The technique used here to obtain  $\Delta H_\alpha$  is that of time-temperature superposition, and before describing experimental results it is pertinent to review the principle of superposition.

\*Present address: Department of Electronics and Electrical Engineering, The University, Glasgow, Scotland.

## 2. Time-temperature superposition

Time-temperature superposition, in which relaxation data measured at one temperature may be shifted along the log time (or log frequency) axis in order to fit data measured at some other temperature, has been known for many years [13] and applied successfully to numerous polymers [14]. The relaxation behaviour of a polymer is governed by the temperature dependence of the distribution of relaxation or retardation times  $\tau$ , usually expressed on a logarithmic time scale [14]. For creep, for example, this is the distribution of retardation times at temperature  $T$ ,  $L_J^T(\ln \tau)$ . More convenient is to consider normalized distributions by dividing by the relaxation magnitude ( $J_R^T - J_U^T$ ). Thus for creep the normalized distribution of retardation times  $\phi_J^T(\ln \tau)$  is just  $L_J^T(\ln \tau)/(J_R^T - J_U^T)$  where  $J_R^T$  and  $J_U^T$  are relaxed and unrelaxed creep compliances at temperature  $T$ . Then  $\phi_J^T(\ln \tau) d \ln \tau$  is simply the fraction of relaxation times between  $\ln \tau$  and  $\ln \tau + d \ln \tau$  at temperature  $T$ . A powerful hypothesis is that as the temperature is changed from  $T_0$  to  $T$  the shape of  $\phi_J^T$  does not change, but each element has its  $\tau$  altered by a temperature-dependent factor  $a_T$  such that

$$\phi_J^T(\ln \tau) = \phi_J^{T_0}(\ln \tau/a_T) \quad (1)$$

where  $\phi_J^{T_0}$  refers to the distribution at temperature  $T_0$  with reduced times  $\tau/a_T$ . When relaxation data are plotted with a logarithmic time (or frequency) axis this factor now appears as  $\ln a_T$  and is just the horizontal displacement needed to superpose data for temperature  $T$  onto that for  $T_0$  to form a "master curve". For a glass-rubber relaxation the horizontal shift is given by the W L F equation [15], but for practically all other relaxations in polymers an Arrhenius relation is found, namely

$$\ln a_T = \frac{\Delta H}{R} \left( \frac{1}{T} - \frac{1}{T_0} \right) \quad (2)$$

from which the activation energy  $\Delta H$  for the relaxation may be determined. ( $R$  is the gas constant.)

As the temperature is changed the shape of  $\phi_J^T$  may not change, but a relaxation still depends on the limiting compliances (or moduli) which are dependent on temperature. Following McCrum and Morris [16], the unrelaxed and relaxed compliances at temperature  $T$  are related to those at  $T_0$  by  $J_U^T = c_T J_U^{T_0}$  and  $J_R^T = d_T J_R^{T_0}$ , where  $c_T$  and  $d_T$  are arbitrary functions

of temperature. Creep compliance curves  $J(t, T)$  measured at  $T$  will superpose onto that for  $T_0$  by the reduction equation ([1], Equation 4.112).

$$J(t/a_T, T_0) = J(t, T) \frac{(J_R^{T_0} - J_U^{T_0})}{d_T J_R^{T_0} - c_T J_U^{T_0}} + \frac{J_U^{T_0} J_R^{T_0} (d_T - c_T)}{d_T J_R^{T_0} - c_T J_U^{T_0}} \quad (3)$$

where it is assumed that each element of  $L_J^T(\ln \tau)$  at temperature  $T$  is related to that at temperature  $T_0$  by a constant factor  $b_T$  given by [16]

$$b_T = \frac{L_J^T(\ln \tau)}{L_J^{T_0}(\ln \tau/a_T)} = \frac{J_R^T - J_U^T}{J_R^{T_0} - J_U^{T_0}} = \frac{d_T J_R^{T_0} - c_T J_U^{T_0}}{J_R^{T_0} - J_U^{T_0}} \quad (4)$$

The general creep reduction equation (Equation 3) can be simplified to

$$J(t/a_T, T_0) = \frac{1}{b_T} J(t, T) + \frac{(d_T - c_T) J_*}{b_T} \quad (5)$$

where  $J_*$  is defined as

$$J_* = \frac{J_U^{T_0} J_R^{T_0}}{J_R^T - J_U^{T_0}} \quad (6)$$

Similarly, the storage and loss compliances may be expressed as [16]

$$J'(a_T \omega, T_0) = \frac{1}{b_T} J'(\omega, T) + \frac{(d_T - c_T) J_*}{b_T} \quad (7)$$

$$J''(a_T \omega, T_0) = \frac{1}{b_T} J''(\omega, T) \quad (8)$$

where  $\omega$  is the frequency. Equations 5, 7 and 8 show that if the limiting compliances are independent of temperature ( $c_T = d_T = b_T = 1$ ) superposition of creep and dynamic compliances will be possible by simply applying a horizontal shift  $\ln a_T$ . However, it is clear that in general  $J_U$  and  $J_R$  are dependent on temperature so that the above full reduction equations should be used. This means that before attempting superposition,  $J_U^{T_0}$  and  $J_R^{T_0}$  must be known together with values of  $c_T$  and  $d_T$ . For the glass-rubber relaxation in an amorphous polymer,  $d_T$  is known explicitly from rubber elasticity theory and is just  $\rho_0 T_0 / \rho T$ , where  $\rho_0$  and  $\rho$  are the specimen densities at temperatures  $T_0$  and  $T$  respectively. Data can then be corrected prior to superposition as, for example, for  $J'(\omega, T)$  curves in polyisobutylene [17]. But for all other relaxations in both amorphous and crystalline polymers there are no rigorous theories for the

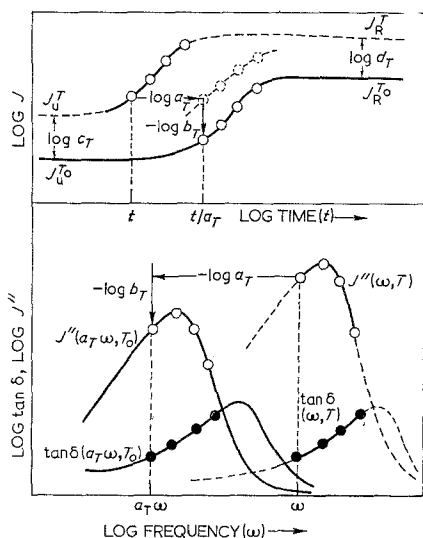


Figure 1 Schematic superposition of creep curves  $J(t, T)$ , loss compliance curves  $J''(\omega, T)$  and loss tangent curves for the case  $c_T = d_T = b_T = 1$  and  $T > T_0$ . (Note plots are double logarithmic.)

temperature dependences of  $J_U$  and  $J_R$ . One solution to the problem is to make the simplifying assumption that the limiting compliances have the same temperature dependence, that is  $c_T = d_T (= b_T) \neq 1$ . Then Equation 5 for creep reduction can be written,

$$\log J(t/a_T, T_0) = \log J(t, T) - \log b_T. \quad (9)$$

This states that when compliances are plotted against time (or frequency) on a log-log plot, a correction factor,  $\log b_T$ , should be made to the data, equivalent to a vertical shift, before superposition can be obtained by a horizontal shift. This is illustrated in Fig. 1. If either  $c_T$  or  $d_T$  is known, then this vertical correction can be applied. For the  $\beta$ -relaxation in polymethylmethacrylate (PMMA) McCrum and Morris [16] assumed that the temperature dependence of the high frequency ( $\sim 10^4$  Hz) modulus [18] of PMMA is just the temperature dependence of the unrelaxed modulus. This gave values for  $1/c_T$  and, hence, the vertical shift correction to the creep compliance was made since it was assumed that  $b_T = d_T = c_T$ . By making this correction [16], the creep data superposed to give an activation energy that agreed with the value obtained from internal friction measurements (location of the loss peak as a function of frequency), while without vertical correction no such agreement is possible.

However, the ultra-sonic technique is not always possible since the temperature dependence of the high frequency modulus will, in general, be a function of other relaxations present at lower temperatures. If neither  $c_T$  nor  $d_T$  is known, then superposition has been obtained by applying in conjunction with the horizontal shift an empirical shift,  $\log b_T$  (Equation 9) in order to give the smoothest possible master curve. Thus, it was shown [19] that for the  $\gamma$ -relaxation in polytetrafluoroethylene a vertical shift of the creep data was necessary to give an activation energy in agreement with the internal friction value.

Although obviously not rigorous, empirical shifting of relaxation data to give a "best-fit" to the master curve can be justified if the  $\Delta H$  value so obtained agrees with less subjectively determined values, as for PMMA [16] and PTFE [19]. For the  $\alpha$ -relaxation in POM, superposition by empirical shifting is the only recourse since the possible presence of  $\beta$ ,  $\gamma$ ,  $\delta$  and  $\epsilon$  relaxations rules out obtaining  $c_T$  from ultra-sonic measurements. The need for vertical shifting for the  $\alpha$ -relaxation in POM has already been established by Miki *et al* [12]. For shear moduli to superpose these authors found that the vertical shift was an approximately linear function of temperature. This result is just that predicted, if the  $\alpha$ -relaxation is an Okano-type crystalline dispersion [20] controlled by the smearing-out of the intermolecular potential owing to intramolecular lattice vibrations.

An important point to emphasize is that the difficulty of rationalizing empirical vertical shifting is largely removed by considering the superposition of loss tangent data. If  $\tan \delta(\omega, T)$  is plotted against  $\log \omega$  both the phenomenological approach of McCrum and Morris and the Miki/Okano approach give the result [12, 16]

$$\tan \delta(a_T \omega, T_0) = \tan \delta(\omega, T), \quad (10)$$

showing that superposition of  $\tan \delta$  can be obtained by horizontal shifting only (see Fig. 1). This result, for example, follows from dividing Equation 8 by Equation 7 provided, of course,  $c_T = d_T$ . Miki *et al* [12] reported superposition of  $\tan \delta$  in POM according to Equation 10 but there is a great deal of scatter on the "smooth" master curve.

One aim of this paper, therefore, is to re-examine superposition in the region of the  $\alpha$ -relaxation of POM, with good (i.e. low

scatter) experimental creep and dynamic measurements over as wide a range of time and frequency as possible. Thence, hopefully, to resolve the question of the activation energy.

### 3. Experimental

#### 3.1. Specimen preparation

Pellets of polyoxymethylene (Delrin 100) were compression-moulded at a temperature of 195°C and pressure of 2 tons in.<sup>-2</sup> to give sheets of POM measuring 150 × 150 × 6 mm<sup>3</sup>. Specimens were cut from this sheet and carefully machined to fit the clamps of the torsion apparatus. Specimen dimensions were 80 × 10 × 0.8 mm<sup>3</sup>. In order to study the  $\alpha$ -relaxation, which is close to the melting point, it is essential to anneal specimens to stabilize them for working temperatures up to the annealing temperature [21]. POM specimens were annealed with free ends [22] at 160°C in dry nitrogen. This temperature was chosen because the crystallinity (as judged by wide-angle X-ray diffraction) is essentially constant up to this temperature [23]. Specimens were annealed for various times, but the one for which mechanical data are presented was annealed for 6 h, giving a specimen density of 1.429 g cm<sup>-3</sup>, equivalent to a 0.73 mass fraction of crystallinity [24]. Small fragments cut from the end of this specimen were used for differential scanning calorimetry. At 160°C the endothermic level was only a few per cent of the peak level at 182°C. Further, identical DSC traces were obtained when the POM specimen was repeatedly cycled from room temperature to temperatures up to just below 160°C.

#### 3.2. Torsion apparatus

Mechanical measurements on the POM specimen were obtained on a counterbalanced creep apparatus similar to the one described elsewhere [16]. For torsional creep, the specimen is connected to a flat coil suspended between the poles of a permanent magnet. A constant current through the coil delivers a constant torque to the specimen. The apparatus is easily modified into a torsion pendulum by replacing the coil/magnet system with an inertia arm capable of varying the frequency of free oscillation. In both modes the system is counterbalanced with a very slight positive tensile load ( $\sim 5$  g) to prevent specimen buckling. The deflection of the specimen is amplified by an optical lever and recorded on a Graphispot chart

recorder. The specimen is encapsulated in a thermostatically controlled chamber through which is bled a current of dry nitrogen.

#### 3.3. Linearity of POM

Both the creep compliance  $J$  and the dynamic modulus  $G'$  are calculated from the theory for torsion of elastic solids with rectangular cross-section [25]. This theory may only be applied to visco-elastic solids if they are linear, that is, if the measured compliance at any time  $t$  is independent of the stress level. Most polymers are linear only for very low strains. Turner [26] has shown that in tensile creep at room temperature, POM departs from linearity at strains greater than 0.002. In the torsional creep of POM described in this paper, the maximum strain reached was only 0.0004. Linearity of the annealed POM specimen was checked directly by measuring isochronal deflections as a function of coil current (proportional to the stress) for stress levels up to twice those used in actual creep measurements. In all cases the maximum departure from linearity was less than 0.8%.

## 4. Results

#### 4.1. Creep compliance data

The POM specimen, already annealed at 160°C for 6 h, was inserted into the creep apparatus and the system counterbalanced. The temperature was taken up to 155°C, held there for 1 h to relieve residual stresses in the specimen, and then returned to room temperature. Isothermal creep runs were started at 20°C and thence in intervals of about 10°C. The resulting creep compliances, corrected for thermal expansion [24], are shown in Fig. 2 as  $\log_{10} J(t, T)$  plotted against  $\log_{10} t$ . The creep times varied from 4½ h below 60°C down to 1 h at the higher temperatures. Further creep measurements (not shown) were then made on the POM specimen at intermediate temperatures by cooling in 10°C intervals down to room temperature. As with the heating measurements, only short creep times (1 h) were used above 100°C, but longer times were used (up to 9 h) at lower temperatures.

After completion of each creep run, the stress was removed and the specimen allowed to recover at the next temperature. Complete recovery is often an asymptotic ideal in a polymer when very long creep times are involved. The criterion used for judging when recovery was *effectively* complete was to wait until the

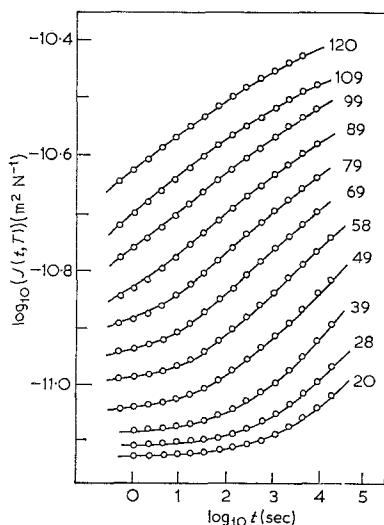


Figure 2 Creep compliance curves for POM,  $\log_{10} J(t, T)$  plotted against  $\log_{10} t$ , for the temperatures indicated ( $^{\circ}\text{C}$ ).

recorder recovery trace was within 1 mm of the baseline (typically, 99% recovery). If the recovery trace showed no detectable shift towards the baseline after a further time of  $\frac{1}{10}$  the next anticipated creep time, then the creep run was started. For the creep data of Fig. 2 this means, at worst, a baseline error in  $J$  of only about 0.5%. Using this recovery criterion, creep strains were recovered in times varying from between 8 and 22 times the previous creep time (that is, recovery times of between 8 h at  $120^{\circ}\text{C}$  and 8 days at  $44^{\circ}\text{C}$ ).

A crucial test of the reliability of the creep data is to examine the reproducibility of the compliance curves at sample temperatures over the range of the creep experiment. Repeated cycles of creep and recovery showed that creep isotherms could be duplicated to within less than 1%, provided effective recovery had occurred.

However, experimental scatter of the measured data points can still prevent any attempt to obtain accurate superposition. Fluctuations in specimen temperature and the applied "constant" coil current are demonstrably minimal. Actual scatter is best assessed by examining isochronal cross-plots, that is,  $J(t_0, T)$  plotted against temperature. The compliance data of Fig. 2 do, in fact, fall on smooth isochronal curves with negligible scatter.

## 4.2. Torsion pendulum data

The torsion apparatus was also used as a pendulum to measure the dynamic mechanical properties of the same POM specimen in the  $\alpha$ -relaxation region. Measurements of the dynamic storage modulus  $G'(\omega, T)$  and loss tangent  $\tan \delta(\omega, T)$  were made at the same  $5^{\circ}\text{C}$  intervals as for the creep data. The range of frequencies covered by the pendulum was from 8 Hz down to 0.6 Hz. From the  $\tan \delta$  and  $G'$  data, the loss compliances,  $J''(\omega, T)$ , were calculated using the Struik equations [27].

Frequency-temperature superposition of the pendulum data by itself is not possible for such a restricted region of the frequency spectrum as barely one decade of  $\log_{10} \omega$ . Accurate superposition of dynamic data would require apparatus capable of varying the frequency over four decades of  $\log \omega$ . Now the  $\alpha$ -relaxation in POM is at its maximum loss at about  $135^{\circ}\text{C}$  at 1 Hz, while above  $160^{\circ}\text{C}$  the crystallinity is known to drop rapidly as the temperature approaches the melting point ( $185^{\circ}\text{C}$ ). Thus, to investigate the relaxation over four decades, and yet be free from the complicating effects of partial melting, it is necessary to use very low frequencies, say from 1 Hz down to 0.0001 Hz. The only practical way to obtain dynamic compliances at such frequencies is by calculation from the equivalent creep compliances.

## 4.3. Conversion of creep data into dynamic data

Of the many approximation methods quoted in the literature for the interconversion of transient and dynamic visco-elastic data, the one used here is that of Struik and Schwarzl [28]. The dynamic shear storage compliance  $J'(\omega)$  and loss compliance  $J''(\omega)$  at a frequency  $\omega (= 1/t)$  are calculated from the creep compliance data  $J(t)$  using the equations

$$J'(\omega) = J(t) + 0.099 [J(8t) - J(4t)] - 0.608 [J(4t) - J(2t)] - 0.358 [J(t) - J(t/2)] \quad (11)$$

$$J''(\omega) = -0.470 [J(4t) - J(2t)] + 1.715 [J(2t) - J(t)] + 0.902 [J(t/2) - J(t/4)]. \quad (12)$$

The Schwarzl-Struik formulae are particularly useful because upper and lower bounds to the relative errors of conversion are also known [28]. Using the three term approximations of Equations 11 and 12 means that the values of  $J'(\omega)$

calculated from the creep data are accurate to within less than  $\pm 1\%$ , while the  $J''(\omega)$  values are accurate to between  $-9$  and  $+2\%$  of the true values.

The entire creep compliance data  $J(t, T)$  were converted to dynamic data  $J'(\omega, T)$  and  $J''(\omega, T)$  together with  $\tan \delta(\omega, T)$  obtained from  $J''/J'$ . Since the calculated dynamic compliances at any frequency  $\omega (=1/t)$  depend on five measured values of creep compliances in the time interval  $t/4$  to  $8t$ , the effective range of  $\log_{10} \omega$  is down by about a decade from the range of  $\log_{10} t$  from which it is derived.

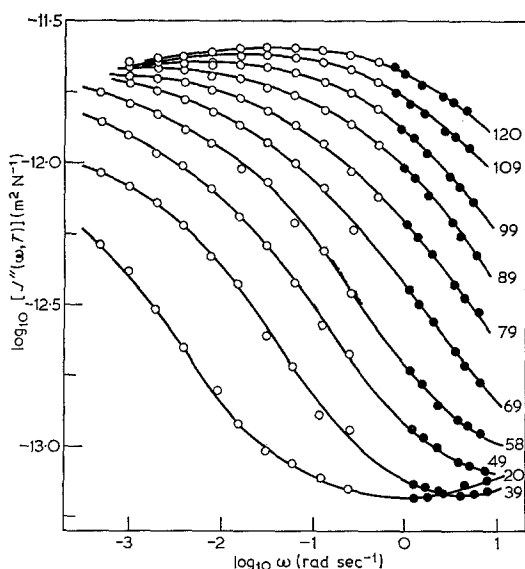


Figure 3 Loss compliance curves for POM,  $\log_{10} J''(\omega, T)$  plotted against  $\log_{10} \omega$ , for the temperatures indicated. Torsion pendulum values (●); calculated values (○).

As an example, the loss compliances for POM at temperatures over the heating cycle are shown in Fig. 3 as  $\log_{10} J''$  plotted against  $\log_{10} \omega$ . The solid symbols refer to direct measurements of  $J''$  with the torsion pendulum and the open symbols to the calculated values. The agreement between the two is particularly good, and means that the total effective range of  $\log \omega$  covered is now  $4\frac{1}{2}$  decades at low temperatures, and a still useful  $3\frac{1}{2}$  decades at higher temperatures. The calculated and measured  $J''$  for the intermediate temperatures obtained upon cooling are also in excellent agreement. The loss tangent data are shown in Fig. 4 as  $\log_{10} \tan \delta$  plotted against  $\log_{10} \omega$ . Again the measured pendulum values

(solid symbols) are in good agreement with those calculated from the creep curves (open symbols).

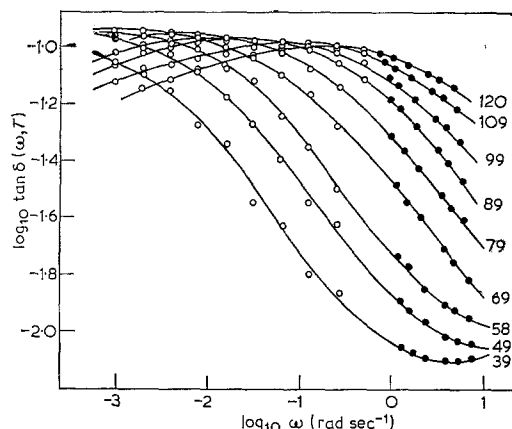


Figure 4 Loss tangent curves for POM,  $\log_{10} \tan \delta(\omega, T)$  plotted against  $\log_{10} \omega$ , for the temperatures indicated. Torsion pendulum values (●), calculated values (○).

#### 4.4. Superposition of the results

Superposition of the POM creep compliance curves  $J(t, T)$  was first attempted by horizontal shifting only (implying that  $c_T = d_T = b_T = 1$ ). This fails to produce any master curve at all, thus agreeing with Miki *et al* [12] that some vertical shifting is needed. Having the  $J(t, T)$  data on a log-log plot allows for superposition assuming  $c_T = d_T = b_T \neq 1$ . Both horizontal shifts ( $\log a_T$ ) and vertical shifts ( $\log b_T$ ) are applied to each creep isotherm so as to give a smooth master curve. That is, Equation 9 again,

$$\log J(t/a_T, T_0) = \log J(t, T) - \log b_T. \quad (13)$$

The results for creep superposition in POM are shown in Fig. 5 with  $20^\circ\text{C}$  as the reference temperature  $T_0$  (for clarity not all the isotherms have been included). The upper master curve (marked I) is the result of superposing each isotherm by combined horizontal and vertical shifting so as to give the best "fit" over the entire experimental time scale (method I). The lower curve (marked II) is the result of superposition by ensuring a best "fit" for only the short time portion of each creep isotherm (method II). Taking Fig. 5. I first, it is noticeable that the master curve is very smooth at short reduced times but shows considerable scatter at long reduced times. The onset of this scatter appears at about  $70^\circ\text{C}$ . Such scatter is somewhat sur-

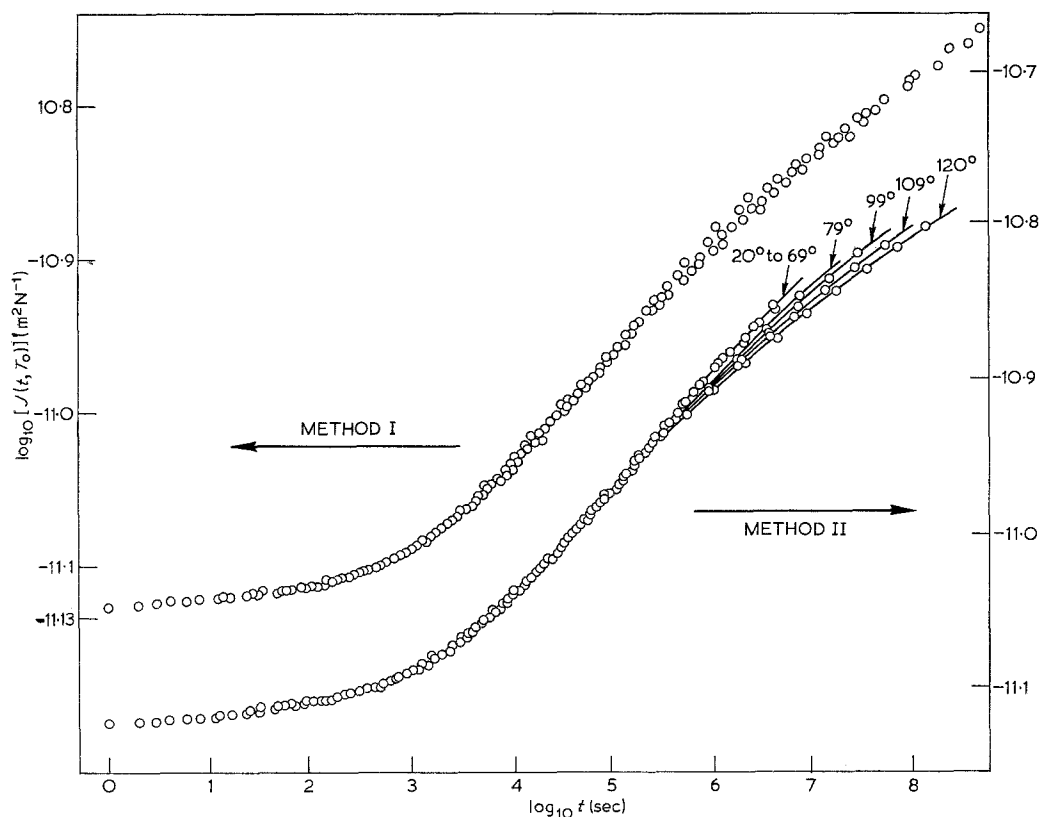


Figure 5 Creep compliance master curves for  $T_0 = 20^\circ\text{C}$ : I (best fit over entire creep time), II (best fit over short time only).

prising since the raw data were carefully checked for reliability and show practically no isochronal scatter over the entire superposition range. When the same creep data are superposed by method II (short time fit) the master curve (Fig. 5, II) is again only smooth up to about  $70^\circ\text{C}$ . Below this temperature the long time points fall onto the same curve as the short time points. Above  $70^\circ\text{C}$  only the short time data can be made to fall onto the  $20^\circ\text{C}$  master curve; the long time portions of successive isotherms deviate from the master curve by increasing amounts. Clearly something is happening above  $70^\circ\text{C}$ ; superposition using the reduction Equation 13 is not sufficient to account for creep above this temperature.

Superposition of the loss compliance data  $J''(\omega, T)$  was also carried out by combined horizontal and vertical shifting on a log-log plot. Equation 8 then becomes

$$\log J''(a_T \omega, T_0) = \log J''(\omega, T) - \log b_T. \quad (14)$$

The resulting loss compliance master curve for

$T_0 = 44^\circ\text{C}$  is shown in Fig. 6. Notice that although the overall scatter is greater than that for creep superposition, this scatter is common to the entire master curve and not to any particular region of the time scale. This is understandable, since the data shown in Fig. 6 comprise not only measured  $J''$  curves but also those calculated from Equation 12 with its concomitant conversion errors [28]. However, the reduction Equations 13 and 14 show that the vertical shifts for superposition of  $J(t, T)$  and  $J''(\omega, T)$  should be identical, that is, the values of  $b_T$  (or  $\log b_T$ ) are the same in both cases. The empirical vertical shifts are plotted in Fig. 7 as a function of temperature for a  $T_0$  of  $20^\circ\text{C}$ . Below about  $70^\circ\text{C}$  there is good agreement between the values of  $b_T$  obtained from superposition of  $J(t, T)$  data by methods I( $\square$ ) and by method II( $\circ$ ) and also from superposition of  $J''(\omega, T)$  data ( $\triangle$ ). Above  $70^\circ\text{C}$ , the  $b_T$  values for creep (I and II) are obviously different (by virtue of the different fitting criteria), and

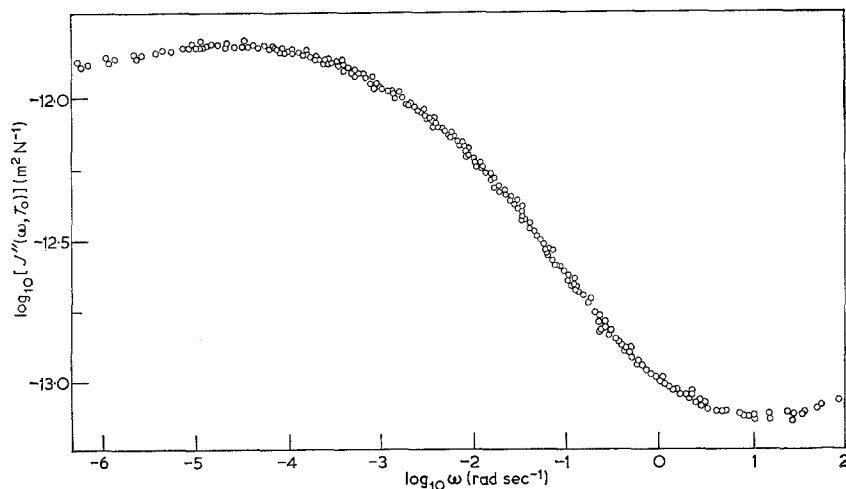


Figure 6 Loss compliance master curve for  $T_0 = 44^\circ\text{C}$ .

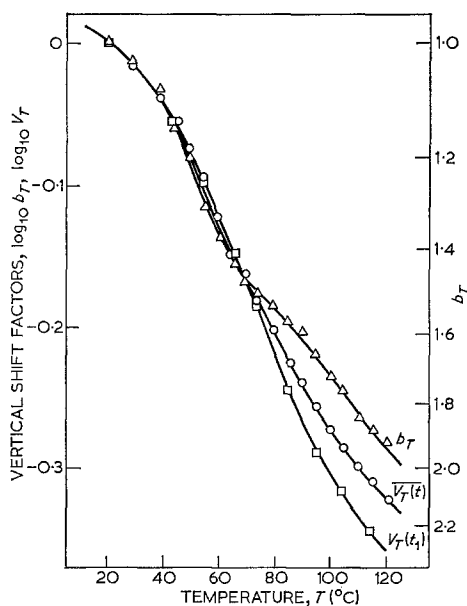


Figure 7 Vertical shift factors  $\log_{10} V_T$  plotted against temperature from superposition of creep curves I(□), II(O) and loss compliance curves ( $\Delta$ ) for  $T_0 = 20^\circ\text{C}$ .

neither agrees with the  $b_T$  values obtained from  $J''$  superposition.

## 5. Discussion

### 5.1. An explanation of the anomalous superposition behaviour

Superposition of creep and loss compliance data in POM has shown that reduction according to

Equations 13 and 14 is no longer an adequate description of the  $\alpha$ -relaxation above about  $70^\circ\text{C}$ . These equations fail for two reasons: (i) the creep curves do not form a single master curve above  $70^\circ\text{C}$ , whereas the  $J''$  curves show no such anomaly (ii) the vertical shift factors for creep (I or II) are inconsistent with those for  $J''$  superposition. However, discontinuities in superposition master curves have been reported before in crystalline polymers [29, 30].

In polytetrafluoroethylene (PTFE) [29] there is a break in the stress relaxation master curve around room temperature but this is caused by the first-order phase transition at  $19^\circ\text{C}$ . In slow-cooled specimens of linear polyethylene (LPE) McCrum and Morris [30] found a distinct break in the creep master curve about 2000 sec ( $T_0 = 20^\circ\text{C}$ ); below about  $50^\circ\text{C}$  the creep data form one master curve, while above  $50^\circ\text{C}$  they form another master curve, yet the two cannot be made to fit together [see Fig. 10, ref. 30]. However, for quenched specimens of LPE no such break is observed. For LPE there is good evidence for at least two relaxations ( $\alpha$  and  $\alpha'$ ) above room temperature. At 0.67 Hz the  $\alpha$ -relaxation has a loss peak at about  $80^\circ\text{C}$  while the  $\alpha'$ -relaxation is manifest at about  $110^\circ\text{C}$  either by a distinct loss peak or as a high temperature "shoulder" [30]. Now the  $\alpha'$ -relaxation is much more pronounced in slow-cooled LPE than in quenched LPE, and it is clear that the break in the creep master curve is caused in some way by the presence of this additional higher temperature relaxation. McCrum and



Morris [30] suggested that a specific mechanism for this  $\alpha'$ -relaxation (namely, lamellar boundary slip) is the reason for the discontinuity in the master curve. However, Thornton [31] concludes that such a discontinuity is to be expected whenever there is an overlap of two relaxations (regardless of the mechanism), provided that they have different activation energies. For the case of LPE, the break occurs simply because  $\Delta H_\alpha = 30 \text{ kcal mol}^{-1}$  and  $\Delta H_{\alpha'} = 24 \text{ kcal mol}^{-1}$  [31].

In contrast to PTFE or LPE, the creep master curve for POM (Fig. 5.II) does not show a distinct split into two separate master curves, rather a whole series of curves. Above  $70^\circ\text{C}$  each creep curve superposes at short times (method II) but at long times the compliances fall below their expected values. That the long time compliance seems too low would suggest that the  $70^\circ\text{C}$  anomaly is not caused by pre-melting, since this should cause each creep compliance to be higher than expected. Further, there is no first order transition in this region (as in PTFE), nor is there any clear evidence for an overlapping relaxation (as in LPE). For the POM specimen studied here, the loss tangent at 0.67 Hz rises from  $20^\circ\text{C}$  to a peak at about  $130^\circ\text{C}$  and then falls symmetrically at least up to  $160^\circ\text{C}$  (the annealing temperature). Of course, this does not rule out the possibility of another relaxation at 0.67 Hz occurring above  $160^\circ\text{C}$ . Read and Williams [6] reported that at 0.3 Hz the  $\alpha$  loss peak in POM is at about  $115^\circ\text{C}$ , but that after falling symmetrically until  $157^\circ\text{C}$  the loss (as measured by the logarithmic decrement) rises again up to the melt at about  $180^\circ\text{C}$ . However, there is no additional loss modulus peak in this region; after the  $\alpha$  peak at about  $90^\circ\text{C}$ ,  $G''$  continues to fall right up to the melt [6]. By reducing the frequency a higher temperature relaxation might manifest itself, but the  $\tan \delta$  curves of Fig. 4 show no sign of any other loss peaks. Cross-plots of  $\tan \delta$  versus temperature for an effective frequency of 0.0002 Hz shows the loss peaks at about  $70^\circ\text{C}$  and then falls continually at least up to  $120^\circ\text{C}$ . The rise in log decrement above  $157^\circ\text{C}$  reported by Read and Williams [6] could more likely arise from the rapid fall in the storage modulus as the crystalline segments start to melt. If there is no strong evidence for believing that the  $\alpha$ -relaxation in POM overlaps with some other high temperature relaxation, then an alternative explanation for the anomalous superposition

results should be sought. One obvious explanation is that the assumption that the limiting compliances have equal temperature dependences ( $c_T = d_T$ ) is no longer valid above  $70^\circ\text{C}$ , so that the full McCrum-Morris reduction Equation (5) should be used.

If  $J_U$  and  $J_R$  do have different temperature coefficients ( $c_T \neq d_T$ ) the creep reduction Equation (5) can be rewritten as

$$\log J(t/a_T, T_0) = \log J(t, T) + \log V_T(t) \quad (15)$$

where

$$\log V_T(t) = -\log b_T - \log [1 + (c_T - d_T)J_*/J(t, T)] \quad (16)$$

The vertical shift  $\log V_T$  is now no longer equal to  $-\log b_T$ . The extra term of Equation 16 involves the compliance  $J(t, T)$  which increases monotonically with time, so that the overall vertical shift for correct superposition should now be time dependent, that is having different values along the creep curve. In a similar fashion, the full reduction of dynamic storage compliance data (Equation 7) becomes

$$\log J'(a_T\omega, T_0) = \log J'(\omega, T) + \log V_T(\omega) \quad (17)$$

where

$$\log V_T(\omega) = -\log b_T - \log [1 + (c_T - d_T)J_*/J'(\omega, T)] \quad (18)$$

These are the frequency analogues of Equations 15 and 16 in which superposition of  $J'(\omega, t)$  data may require a frequency dependent vertical shift different from  $\log b_T$ . However, it is important to note that the loss compliance data  $J''(\omega, T)$  according to Equation 8, will superpose with a constant (i.e. frequency independent) vertical shift  $\log b_T$  regardless of whether  $c_T$  is greater than, equal to or less than  $d_T$ .

The master curves of Fig. 6 can now be explained if the  $\alpha$ -relaxation in POM is such that  $c_T > d_T$  above  $70^\circ\text{C}$ . Equation 16 means that superposition of creep data at experimentally short times ( $t_1$ ) will require a vertical shift  $\log V_T(t_1)$  which is greater than the vertical shift  $\log V_T(t_2)$  at experimentally long times ( $t_2$ ). Creep superposition by method I (fit over entire time scale  $t_1$  to  $t_2$ ) yields a vertical shift that is some average of  $V_T(t_1)$  and  $V_T(t_2)$  so that in a region where  $c_T \neq d_T$  there will be poor superposition. Creep superposition by method II (short time fit) will yield a vertical shift  $\log V_T(t_1)$  so that above  $70^\circ\text{C}$  the long time regions of the measured creep curves fail to superpose because too large a vertical shift has been applied. This effect is seen more clearly in Fig. 7 in which

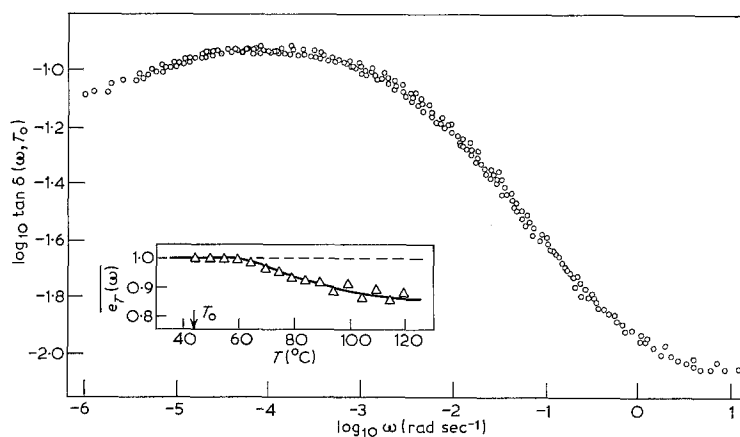


Figure 8 Loss tangent master curve for  $T_0 = 44^\circ\text{C}$ . The inset is a plot of  $\bar{e}_T(\omega)$ .

the vertical shift for  $J''$  superposition ( $b_T$ ) agrees with that for superposition only below  $70^\circ\text{C}$  (for which  $c_T = d_T$ ). Above  $70^\circ\text{C}$  the effect of  $c_T > d_T$  is to make the average vertical shift factor  $\log V_T(t)$  of method I, or the short time vertical shift factor  $\log V_T(t_1)$  of method II, both greater than  $\log b_T$  because of the extra term  $\log[1 + (c_T - d_R)J_*/J(t, T)]$  in Equation 16. Note that if  $c_T < d_T$  these effects are reversed. Then  $b_T > d_T > c_T$ , so that  $J''$  vertical shift factors will exceed creep vertical shift factors and type II creep superposition will cause long time data to fall above the master curve instead of below it.

More interesting is the effect of  $c_T \neq d_T$  on the superposition of loss tangent data  $\tan \delta(\omega, T)$ . By dividing Equation 8 by Equation 7, and after some manipulation, we can write

$$\log \tan \delta(a_T \omega, T_0) = \log \tan \delta(\omega, T) + \log e_T(\omega) \quad (19)$$

where

$$\log e_T(\omega) = \log [1 + (c_T - d_T)J_*/J'(\omega, T)]. \quad (20)$$

If, as is commonly assumed, the limiting compliances do have the same temperature dependences ( $c_T = d_T$  for all  $T$ ) then  $\tan \delta$  plotted against  $\log \omega$  will superpose by horizontal shift  $\log a_T$ , but no vertical shift ( $e_T = 1$ ). Equation 19 then reverts to Equation 10. But if  $c_T \neq d_T$  superposition will also need a frequency-dependent vertical shift  $\log e_T(\omega)$ . If  $c_T > d_T$  ( $T > T_0$ ) the shift will be upward along the  $\log \tan \delta$  axis. If  $c_T < d_T$  then the shift will be downward. Thus the self-consistency of this explanation ( $c_T > d_T$ ) can be checked by superposing the  $\tan \delta(\omega, T)$  data of Fig. 4.

The results are shown in Fig. 8. Up to  $70^\circ\text{C}$  only horizontal shifting is required ( $e_T = 1$ ), reaffirming that  $c_T = d_T$ . Above  $70^\circ\text{C}$  the loss isotherms can only be made to superpose onto the master curve ( $T_0 = 44^\circ\text{C}$ ) by a small upward vertical shift corresponding to some average value  $\log \bar{e}_T(\omega)$ . (Plotted in the inset are the observed  $\bar{e}_T(\omega)$  values.) The overall scatter is fairly large (again owing to conversion errors in calculating  $\tan \delta$  rather than from the torsion pendulum values) but the need for vertical shifting is perhaps more obvious in Fig. 4; for example the loss peak for  $120^\circ\text{C}$  is some 12% lower than that for  $58^\circ\text{C}$ .

A similar effect should, in principle, be observed for  $\tan \delta$  in amorphous polymers, since  $c_T \neq d_T$  for a glass-rubber relaxation. The temperature dependence of  $J_R$  is known from theory,  $d_T (= \rho_0 T_0 / \rho T) < 1$  for  $T > T_0$ . The temperature dependence of  $J_U$  is not known, but good superposition was reported [17] by ignoring any dependence, that is  $c_T = 1$ , making  $c_T > d_T$  as in POM. Measurements on polyvinyl chloride [32] show that  $\tan \delta$  versus  $\log \omega$  curves for the glass-rubber relaxation do indeed show maxima that become progressively smaller as the temperature increases (just as in Fig. 4) and superposition would not be possible by horizontal shifting alone.

The results of  $J, J''$  and  $\tan \delta$  superposition in POM are all consistent with the conclusion that below about  $70^\circ\text{C}$   $c_T = d_T$  while above  $70^\circ\text{C}$   $c_T$  gradually increases more rapidly than  $d_T$ . However, implicit in these conclusions is the assumption that the shape of the normalized distribution of retardation times  $\phi_{J''}(\ln \tau)$  does

not change, that is, Equation 1 is always obeyed. This assumption is central to the superposition phenomenon, and the question that naturally arises is what happens if the assumption is not justified; is not a simpler explanation of the creep results that above 70°C Equation 1 is no longer true?

Reference to Fig. 5 shows that measured creep curves at high temperatures have mean slopes  $d \log J/d \log t$ , that are too small to superpose onto the  $T_0$  master curve – they are just too flat. The explanation that  $c_T > d_T$ , but  $\phi_{J^T}(\ln \tau)$  obeys Equation 1, means full superposition can only be achieved by time-dependent vertical shifts  $\log V_T(t)$ . The alternative to this, that  $\phi_{J^T}(\ln \tau)$  does not obey Equation 1, regardless of whether  $c_T = d_T$  or not, means superposition requires time-dependent horizontal shifts  $\log a_T(t)$ . Such shifts have been proposed for “thermo-rheologically complex” materials such as polymer blends and tri-block co-polymers [33]. For these materials,  $\log a_T(t)$  is a function of time (as well as temperature) because of the different time/temperature regimes of the component relaxations.

For a homopolymer such as POM time-dependent horizontal shifting could still arise in two cases: (a) when there is overlap of different distributions and of different activation energies as implied by Thornton [31] and (b) when there is a single distribution but whose retardation times shift non-uniformly along the log time axis, i.e.  $\Delta H_\alpha$  depends on  $\tau$ . In both cases the shape of the overall distribution will no longer remain constant and superposition will be impossible. If  $\log a_T(t)$  shifting were operable Fig. 5 shows that the high temperature creep curves need smaller shifts at long times than at short times, that is  $a_T(t_2) < a_T(t_1)$ . If (a) were the case in POM the activation energy of the (unresolvable) higher temperature relaxation should be less than that of the lower temperature relaxation. Such is the case for LPE [30, 31] for which  $\Delta H_{\alpha'} < \Delta H_{\alpha''}$ , but, as will be shown in the next section, if a higher temperature relaxation is present in POM it has a higher  $\Delta H$  rather than a lower one. If (b) were the case, some peculiar mechanism is required to explain  $\Delta H(\tau)$ . In either case, however, if  $\phi_{J^T}(\ln \tau)$  does not obey Equation 1 and this is used to explain the creep anomaly, then it cannot also explain why  $J''$  superposes successfully, nor why  $\tan \delta$  superposition needs a vertical shift. The ineluctable conclusion is that the explanation of the results

in terms of  $c_T > d_T$  is the only reasonable one.

## 5.2. The activation energy

Up to now no mention has been made of the measured horizontal shift factors  $\log a_T$ . If the  $\alpha$ -relaxation is a rate-activated process then plots of horizontal shift versus reciprocal temperature (in K) should produce a straight line (Equation 2) from which an activation energy,  $\Delta H$ , is calculated. Further, for the same reference temperature  $T_0$ , superposition of creep compliance, loss compliance and loss tangent data should all give the same values of  $a_T$ , and hence of  $\Delta H$ . Fig. 9 shows a plot of  $\log_{10} a_T$  against  $1/T$  K for the superposition of  $J''$  (I and II), and  $\tan \delta$  for a common  $T_0$  of 44°C. This  $T_0$  was chosen because 44°C was the lowest temperature for which there was good agreement between the calculated values of  $\tan \delta$  and those measured with the torsion pendulum.

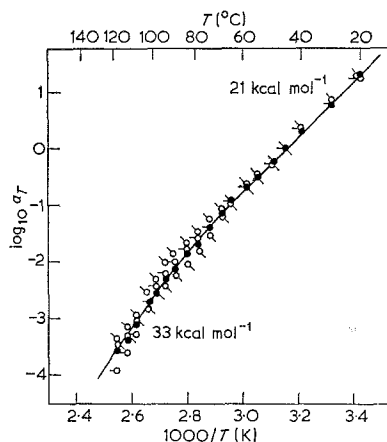


Figure 9 Horizontal shift factors  $\log_{10} a_T$  plotted against reciprocal temperature (K) for superposition of  $J''$  (●) creep I (○), creep II (○) and  $\tan \delta$  (□) for  $T_0 = 44^\circ\text{C}$ . The activation energies indicated refer to the value below 70°C and the value at 120°C.

It is apparent from Fig. 9 that once again the situation at high temperatures is more complicated than at low temperatures. Only in the temperature range 20 to 70°C is there agreement between the four sets of  $a_T$  values, and only in this range is a straight line possible through the data points. This gives an apparent activation energy  $\Delta H_\alpha$  of  $21 \pm 1 \text{ kcal mol}^{-1}$ . Above 70°C there is poor agreement between the  $a_T$  values, and no single straight line through the

data is justifiable. The full curve drawn in Fig. 9 is the best fit to the  $J''$  values ( $\bullet$ ). Type II creep superposition (short time fit) give  $\log_{10} a_T$  values ( $\circ$ ) that are systematically smaller (by up to 14%) than the  $J''$  values. Type I creep superposition (short and long time fit) gives  $\log_{10} a_T$  values ( $\circ$ ) that are slightly closer to  $J''$  values than for type II creep up to about 105°C, but above this they are appreciably greater (20% at 120°C). The  $\tan \delta$  values of  $\log_{10} a_T$  ( $\circ$ ) are in better agreement with  $J''$  values than for creep, although they are systematically slightly larger at intermediate temperatures ( $\sim 5\%$ ).

If the explanation of the superposition anomaly in terms of  $c_T > d_T$  is the correct one, then it makes sense to regard the  $J''$  values of  $a_T$  as the most reliable of the four since good superposition is possible over the entire range 20 to 120°C and no frequency-dependent vertical shift is required even when  $c_T \neq d_T$ . It is for this reason that the full curve in Fig. 9 is drawn through the  $J''$  points. It is not surprising that type II creep values of  $a_T$  are somewhat too small because a constant and too large a vertical shift factor  $\log V_T(t_1)$  was used above 70°C. Slightly better agreement with  $J''$  is obtained from type I creep values because long time data were superposable by an average vertical shift  $\log \overline{V_T}(t)$ , although above 105°C even this method fails. With  $\tan \delta$  superposition, allowing a vertical shift (as an approximation to  $\log e_T$ ) the  $a_T$  values are the closest to the  $J''$  values over the whole temperature range. The full curve drawn through the  $J''$  points implies that at high temperatures the activation energy apparently increases steadily with temperature, from 21 kcal mol<sup>-1</sup> at 70°C up to 33 ( $\pm 2$ ) kcal mol<sup>-1</sup> at about 120°C. It is instructive to compare these values of  $\Delta H_\alpha$  with those taken from the literature.

As mentioned in the introduction, there is a wide range of values quoted in the literature for the activation energy of the  $\alpha$ -relaxation in POM, from 20 to 92 kcal mol<sup>-1</sup>. This is illustrated in Fig. 10, in which  $\Delta H_\alpha$  is plotted against temperature (note the change of scale above 40 kcal mol<sup>-1</sup>). The single symbols ( $\circ$ ) refer to  $\Delta H$  values measured at some particular temperature and joined symbols ( $\circ$ — $\circ$ ) to values for a temperature range. The shaded area represents the results of superposition and clearly incorporates the general trend of other measurements, but there are five notable discrepancies. Two of these can be ignored: (1) the value of 24 kcal

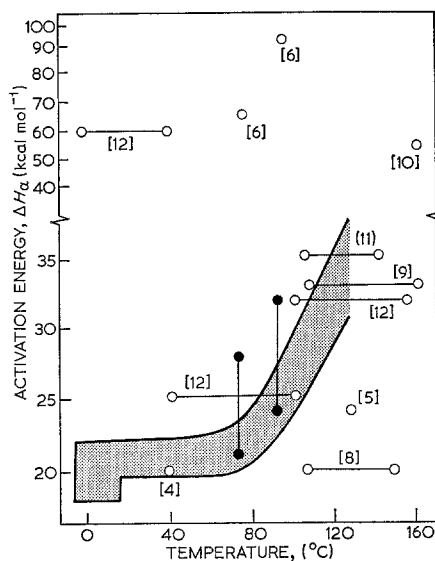


Figure 10 Temperature distribution of the apparent activation energy for the  $\alpha$ -relaxation in POM as measured by various authors. Indicated in parentheses are author reference numbers. The shaded area refers to this paper. The symbols ( $\bullet$ ) are corrected values of [6] (see text).

mol<sup>-1</sup> at 130°C found by McCrum [5] using an elastic after-effect method, is now considered to be unreliable [34]; (2) the value of 20 kcal mol<sup>-1</sup> at about 120°C was found by Arisawa *et al* [8] using dielectric loss measurements in which no account was made for d.c. conduction; the same authors [9] later separated out the relaxation and conduction contributions to the total loss and this gave the more realistic figure of 33 kcal mol<sup>-1</sup> for  $\Delta H$ . Apart from the high  $\Delta H_\alpha$  (55 kcal mol<sup>-1</sup>) found by Takayanagi [10], which was not for bulk POM but from single crystal mats, this leaves just two major discrepancies to be explained, those of Read and Williams [6] and Miki *et al* [12].

The POM specimen used by Read and Williams [6] was very similar to the one used in the present work – both were Delrin homopolymers (though in their case of slightly lower molecular weight, Delrin R 500), both were annealed at 160°C giving closely similar densities (1.429 and 1.434 g cm<sup>-3</sup>). Read and Williams [6] measured storage and loss shear moduli ( $G'$  and  $G''$ ) at two fixed frequencies for temperatures from 20 to 147°C, and by measuring the area ( $A_{G''}$ ) under the  $G''$  versus  $1/T$  curve a value for the activation energy was calculated from the equation [35],

$$\Delta H_{RW} = \left\langle \frac{1}{H} \right\rangle_{av}^{-1} = (G_U - G_R) \frac{R\pi}{2AG''} \quad (21)$$

where  $G_U$  and  $G_R$  are the unrelaxed and relaxed shear moduli and  $(G_U - G_R)$  is assumed to be independent of temperature. Now  $\Delta H_{RW}$  is an average activation energy, averaged over  $\phi_G^T$  ( $\ln \tau$ ) in which the distribution of  $\tau$  ( $=\tau_0 \exp[\Delta H/RT]$ ) can, in general, arise through variations in both  $\tau_0$  and  $\Delta H$  [35]. As such,  $\Delta H_{RW}$  may not be simply relatable to  $\Delta H_\alpha$ , the value obtained from superposition. Read and Williams [6] used Equation 21, taking the measured shear moduli  $G'$  ( $20^\circ\text{C}$ ) and  $G'$  ( $147^\circ\text{C}$ ) as  $G_U$  and  $G_R$  respectively, and obtained values of activation energy  $\Delta H_{RW}$  of 65 and 92 kcal mol $^{-1}$  at 77 and  $94^\circ\text{C}$  respectively (the temperatures of the loss maxima,  $G''_{\max}$  at the two different frequencies). The values are unrealistically high because it is clear from superposition that the limiting compliances and, hence, the limiting moduli are sensitive functions of temperature, and so the assumption that  $(G_U - G_R)$  is independent of temperature is unjustifiable.

It is not possible to derive a general expression for  $\Delta H$  in terms of  $c_T$  and  $d_T$  for the case of temperature dependent limiting moduli, but a realistic approximation is to re-calculate  $\Delta H$  from Equation 21 using  $(G_U^{T''} - G_R^{T''})$  measured at  $T''$ , the temperature of  $G''_{\max}$ , rather than the hybrid value  $(G_U^{20} - G_R^{147})$ . This is analogous to the single relaxation model for dielectrics [35]; for polar media the difference between the limiting dielectric constants  $(\epsilon_U^{T''} - \epsilon_R^{T''})$  varies as the reciprocal of the temperature, and for a single relaxation time the activation energy can be calculated from the dielectric equivalent of Equation 21 using  $(\epsilon_U^{T''} - \epsilon_R^{T''})$  measured at  $T''$ , the temperature for maximum dielectric loss  $\epsilon''_{\max}$  (see Equation 4.83, reference 1). Now  $G_U^T = c_T^{-1} G_U^{T_0}$  and  $G_R^T = d_T^{-1} G_R^{T_0}$  so that for  $T_0 = 20^\circ\text{C}$  a correction to  $\Delta H_{RW}$  can be made, namely,

$$\Delta H^* = \Delta H_{RW} \left[ \frac{c_T^{-1} G'(20^\circ\text{C}) - c_T^{-1} d_{147}^{-1} G'(147^\circ\text{C})}{G'(20^\circ\text{C}) - G'(147^\circ\text{C})} \right] \quad (22)$$

To calculate  $\Delta H^*$  the coefficients  $c_T$  and  $d_T$  at 77 and  $94^\circ\text{C}$  together with  $d_T$  at  $147^\circ\text{C}$  must be known. (Values of  $G'$  ( $20^\circ\text{C}$ ) and  $G'$  ( $147^\circ\text{C}$ ) are obtained from [6].) Because of the similarity between the two POM specimens, it seems not

unreasonable to estimate these coefficients from the current superposition results; the method used is outlined below.

From Equations 4 and 6 coefficients  $c_T$  and  $d_T$  can be written

$$c_T = b_T + (c_T - d_T) J_* / J_U^{T_0} \quad (23)$$

$$d_T = b_T + (c_T - d_T) J_* / J_R^{T_0} \quad (24)$$

The values of  $b_T$  for 77 and  $94^\circ\text{C}$  ( $T_0 = 20^\circ\text{C}$ ) are obtained directly from the  $J''$  vertical shifts of Fig. 7 (right-hand scale). Values of  $(c_T - d_T) J_*$  are obtained from the  $\tan \delta$  vertical shifts of Fig. 8, since from Equation 20

$$(c_T - d_T) J_* \approx (\bar{e}_T(\omega) - 1) \bar{J}'(\omega, T) \quad (25)$$

where  $\bar{e}_T(\omega)$ , the average  $\tan \delta$  vertical shift ( $T_0 = 44^\circ\text{C}$ ), and  $\bar{J}'(\omega, T)$ , the average storage compliance at temperature  $T$ , are known for  $T = 77$ , and  $94^\circ\text{C}$ . (Since  $e_T = 1$  up to  $70^\circ\text{C}$  the  $\bar{e}_T$  values above  $70^\circ\text{C}$  are also those for  $T_0 = 20^\circ\text{C}$ .) Thus all that is required to estimate  $c_T$  and  $d_T$  are values for  $J_U^{T_0}$  and  $J_R^{T_0}$  ( $T_0 = 20^\circ\text{C}$ ), together with  $\bar{J}'(\omega, T)$ ,  $\bar{e}_T$  and  $b_T$  at  $T = 147^\circ\text{C}$ . From the  $20^\circ\text{C}$  master curve of Fig. 5 it is reasonable to take  $\log_{10} J_U^{T_0}$  as  $-11.13$ , or  $J_U^{T_0}$  as  $7.5 \times 10^{-12} \text{ m}^2 \text{ N}^{-1}$ . More difficult is  $J_R^{T_0}$  since the relaxation is clearly not complete, but  $\log_{10} J_R^{T_0}$  from Fig. 5 is probably between  $-10.6$  and  $-10.4$  giving a range for  $J_R^{T_0}$  of 25 to  $40 \times 10^{-12} \text{ m}^2 \text{ N}^{-1}$ . Finally, extrapolation of  $\bar{J}'(\omega, T)$ ,  $b_T$  and  $\bar{e}_T$  curves to  $T = 147^\circ\text{C}$  gives  $d_{147} \cong 2.5 \pm 0.3$ . (Happily  $\Delta H^*$  is not too sensitive to the extrapolation and to the value of  $d_{147}$ .) The results of these corrections are tabulated overleaf.

It is admitted that these corrections are a somewhat crude attempt to allow for temperature dependent limiting moduli, but the resulting ranges of activation energies,  $\Delta H^*$ , are now in much closer agreement to the  $\Delta H_\alpha$  values found from superposition ( $\Delta H^*$  is plotted as filled symbols in Fig. 10).

The other major discrepancy in Fig. 10 concerns the values of activation energy found by Miki *et al* [12] from horizontal (and vertical) shifting of forced oscillation data,  $\log G'(\omega, T)$  and  $\log G''(\omega, T)$ . The polymer used was Delrin 150 X annealed at  $189^\circ\text{C}$  and density  $1.436 \text{ g cm}^{-3}$  (in our case the polymer was Delrin 100, annealed at  $160^\circ\text{C}$  and density  $1.429 \text{ g cm}^{-3}$ ). Miki *et al* [12] found distinct changes of slope on their  $\log a_T$  versus  $1/T$  plots at about 39 and  $95^\circ\text{C}$  and suggested that the  $\alpha$ -relaxation has three components: (i) below  $39^\circ\text{C}$  the value of

Temperature °C)	$b_T^*$	$d_T^*$	$c_T^*$	$\Delta H_{RW}$ (kcal mol <sup>-1</sup> )	$\Delta H^*$
77	1.50	1.52 to 1.53	1.61	65	24 to 28
94	1.65	1.70 to 1.73	1.91	92	26 to 32

\*( $T_0 = 20^\circ\text{C}$ )

$\Delta H_\alpha$  is very large (about 60 kcal mol<sup>-1</sup> as estimated from Fig. 9 reference 12) (ii) between 39 and 95°C  $\Delta H_\alpha$  is 25 kcal mol<sup>-1</sup> and (iii) above 95°C  $\Delta H_\alpha$  is 33 kcal mol<sup>-1</sup>. These conclusions are not in agreement with the present results, that between 20°C and about 70°C  $\Delta H_\alpha$  is approximately constant at  $21 \pm 1$  kcal mol<sup>-1</sup>, but above 70°C  $\Delta H_\alpha$  seems to increase and by 120°C is about  $33 \pm 2$  kcal mol<sup>-1</sup>. No evidence was found for an activation energy below 39°C of 60 kcal mol<sup>-1</sup>. This point was further pursued by making additional torsional creep measurements at subambient temperatures, from 20°C down to -3°C. The resulting 1000 sec creep curves superpose perfectly onto the master curves of Fig. 5 with horizontal shifts  $\log a_T$  that correspond to an  $\Delta H_\alpha$  of  $20 \pm 2$  kcal mol<sup>-1</sup> in the region -3 to +20°C (see Fig. 10). Thus again no evidence for a 60 kcal mol<sup>-1</sup> process was observed at low temperatures. Of course there may be differences in the POM specimens used, but it is felt that the quality of the superposition obtained by Miki *et al* [12] does not justify such a precise demarcation into three discrete regimes. There seems to be considerable scatter of the raw data even before superposition was attempted, and a relatively short frequency scan was used (only  $2\frac{1}{2}$  decades, as opposed to 5 decades here). In this context it is not surprising that the need for a frequency dependent vertical shift was not observed. Miki *et al* [12] also reports that  $\tan \delta$  superposes with horizontal shifts only, but the master curve is by no means "smooth". It should be pointed out that only by taking measurements over 5 decades or so would the extra terms in  $e_T(\omega)$  or  $V_T(t)$  become noticeable.

### 5.3. On the nature of the relaxation

Discussion of the results has led to the conclusion that below about 70°C  $c_T = d_T$  and  $\Delta H_\alpha$  is constant, while above 70°C  $c_T > d_T$  and  $\Delta H_\alpha$  increases with temperature. This raises the all-important question - why? The experiment described in this paper cannot provide a definite answer because the exact mechanism of the

$\alpha$ -relaxation in POM is unclear and no rigorous theory exists for the temperature dependence of the limiting compliances. The final section of the paper is concerned with some general remarks on the behaviour of POM at high temperatures that suggest a possible answer to the above question.

First of all, it should be remembered that superposition is only possible if  $\phi_{J^T}(\ln \tau)$  obeys the constant shape hypothesis (Equation 1). The equivalent statement of this hypothesis is that every element of the actual (unnormalized) distribution  $L_{J^T}(\ln \tau)$  is affected equally by an amount  $b_T$  when the temperature is changed from  $T_0$  to  $T$  (Equation 4). Vertical shifting of  $J''(\omega, T)$  gave good superposition up to 120°C thus confirming this hypothesis. The fact that for creep  $J(t, T)$  also superposes with the same vertical shift factors as for  $J''(\omega, T)$ , at least up to 70°C, strictly only implies that  $c_T \simeq d_T \simeq b_T$ . Above about 70°C the creep anomaly is explained by  $c_T > d_T > b_T$ , without violating Equation 1. There is no clearly defined temperature at which anomalous behaviour starts, and most probably the  $\alpha$ -relaxation is such that  $c_T > d_T > b_T$  over the entire relaxation but that the inequality is only apparent above 70°C.

There is, of course, no *a priori* reason why  $c_T$  should equal  $d_T$ , and hence  $b_T$ . The coefficient  $c_T$  controls  $J_U^T(\alpha)$ , the level of compliance at times prior to the onset of the high temperature  $\alpha$ -relaxation, a relaxation generally accepted to be caused by large-scale co-operative motion of crystalline segments [1]. Since the POM specimens remained free of water during the experiment there is virtually no contribution from the water-sensitive  $\beta$ -relaxation [5] so that  $J_U^T(\alpha)$  is in effect identifiable with  $J_R^T(\gamma)$ , the relaxed compliance for the low temperature amorphous  $\gamma$ -relaxation [5]. Thus  $c_T(\alpha)$  is controlled by the extent to which amorphous chain segments relax in the  $\gamma$ -relaxation. The coefficient  $b_T$  controls the extent to which further relaxation ( $J_R^T - J_U^T$ ) occurs as a result of the  $\alpha$ -relaxation, and is the amount by which each element in the retardation spectrum  $L_{J^T}(\ln \tau)$  is increased when the temperature is increased.

One mechanism for amplifying each element of  $L_J^T$  ( $\ln \tau$ ) in POM has already been proposed by Miki *et al* [12]. These authors found vertical shifts (equivalent to  $\log b_T$ ) that increased linearly with temperature, that is,  $b_T$  has the form  $\exp[\beta(T - T_0)]$  where the coefficient  $\beta$  has the value  $0.94 \times 10^{-2} \text{ }^\circ\text{C}^{-1}$ . This result [12] was taken as support for the interpretation [36] that the high temperature  $\alpha$ -relaxation in all crystalline polymers is owing to incoherent lattice vibrations smearing-out the intermolecular potential [20]. Okano's potential theory [20] leads to a vertical shift factor

$$\exp \left[ \frac{\pi^2 Nk}{5fa^2} (T - T_0) \right]$$

so that  $\beta$  can be identified with  $\pi^2 Nk/5fa^2$ . The terms in this expression for  $\beta$  arise from a loaded string model of polymer chains [37] considered as  $N$  atomic units distant  $a$  apart with force constant  $f$  ( $k$  is the Boltzmann constant). Miki *et al* [12] showed that their measured  $\beta$  ( $0.94 \times 10^{-2} \text{ }^\circ\text{C}^{-1}$ ) yields a reasonable value for  $f$  by taking the X-ray long spacing as a measure of  $a$ . It is significant that in Fig. 7 the vertical shift factor from method II creep superposition also increases approximately linearly with temperature, from about 40 to 120 $^\circ\text{C}$ . The mean slope of this line gives a  $\beta$  value of  $1.0 \times 10^{-2} \text{ }^\circ\text{C}^{-1}$ , close to the Miki value. The Miki/Okano model does offer some justification for why  $b_T$  increases with temperature but it fails to give a satisfactory reason for why  $c_T > d_T$  above about 70 $^\circ\text{C}$ . For example, if short  $\tau$  elements of  $L_J^T$  ( $\ln \tau$ ) were "smeared" more effectively than long  $\tau$  elements, then by definition this demands a larger vertical shift at short creep times than at long creep times (as observed), but it would also mean that the shape of  $\phi_J^T$  ( $\ln \tau$ ) would alter and  $J''$  would not then superpose. Reference to Fig. 7 again shows that above 70 $^\circ\text{C}$  the  $\log b_T$  curve has a mean slope  $\beta$  that is less than at lower temperatures. Of course, this alone does not alter the shape of  $\phi_J^T$  ( $\ln \tau$ ) but nor does it explain why  $c_T > d_T$ . Above about 70 $^\circ\text{C}$  some additional mechanism must cause POM at long times to appear somewhat less compliant than expected. Some insight into this problem may be gleaned from the observations of O'Leary and Geil [38] on small angle X-ray diffraction in POM.

O'Leary and Geil [38] found that specimens of bulk and drawn POM, annealed at 160 $^\circ\text{C}$ , showed large reversible changes in small angle

spacing (SAS) and small angle intensity (SAI) during a subsequent heating and cooling cycle. (Annealing itself produces the usual irreversible increases in SAS and SAI.) As annealed POM is reheated from room temperature the SAS increases very slightly up to 125 $^\circ\text{C}$  and then very rapidly between 125 and 160 $^\circ\text{C}$ . In contrast, the SAI increases steadily over the whole heating range. On cooling from 160 $^\circ\text{C}$  both SAS and SAI decrease and return to their room temperature values, although over the range 90 to 140 $^\circ\text{C}$  the cooling values are slightly greater than the heating values.

It is generally accepted that small angle X-ray scattering in semi crystalline polymers is owing to periodic fluctuations of order in both crystalline and amorphous regions. Various paracrystalline lattice models have been suggested to account for the scattering behaviour at low angles (see Crist [39]) and these can give rise to significant changes in both SAS and SAI. Over the range of superposition (20 to 120 $^\circ\text{C}$ ) the results of O'Leary and Geil [38] for 160 $^\circ\text{C}$  annealed POM show that the small angle X-ray intensity almost doubles; the wide angle X-ray crystallinity, of course, remains constant. One explanation [38] is that SAI increases owing to thickening of the lamellar crystal interior at the expense of the density deficient surface layer [40], while not affecting the total thickness (interior + surface) of the lamellae, and hence the SAS. For example, the number of loose chain folds could be reduced as the temperature increases. If this is the case, and if the  $\alpha$ -relaxation in POM involves motion of both interior chain segments and also chain folds (as proposed [41] for polyethylene) then a qualitative rationale of why  $c_T > b_T$  (and hence  $c_T > d_T$ ) is possible.

The coefficient  $b_T$  that causes ( $J_R^T - J_U^R$ ) and  $L_J^T$  ( $\ln \tau$ ) to increase is dependent on the state of order at the crystal/amorphous interface. The coefficient  $c_T$  that causes  $J_U^T$  ( $\alpha$ ) to increase is dependent on the state of relaxation in the bulk amorphous material and is not affected by the small-angle re-ordering. As re-ordering becomes significant (above about 70 $^\circ\text{C}$ ), a modified  $b_T$  causes POM to relax slightly less than expected while  $c_T$  remains the same, that is  $c_T > b_T$  and  $c_T > d_T > b_T$ . It is realized that this argument is somewhat tentative because (i) the precise mechanism of the  $\alpha$  relaxation in POM is not proven (ii) there is no rigorous theory for the factor  $b_T$  and (iii) the details of the re-ordering are unclear. Obviously further experiments in the

region of the  $\alpha$ -relaxation are needed to resolve these matters.

Finally, some mention should be made about why the activation energy should increase above about 70°C (see Fig. 10). The various models proposed by Hoffman *et al* [41] for the  $\alpha$ -relaxation in polyethylene yield values of  $\Delta H_\alpha$  that are sensitive to the relative thicknesses of the lamellar interior and the fold surface layer. For example,  $\Delta H_\alpha$  for the  $\alpha_c - C_c$  model (relaxation of interior chains) increases with the number of methylene units in the chain. Assuming a similar process occurs in POM, then the reversible lamellar thickening found by O'Leary and Geil [38] will increase the chain interior and so  $\Delta H_\alpha$  would be expected to increase. It is perhaps for this reason that so high a value (50 kcal mol<sup>-1</sup>) for  $\Delta H_\alpha$  is observed [10] for single crystals of POM at about 160°C, in which the overall lamellar thickness may be particularly high.

## 6. Conclusions

1. Superposition of loss compliance curves justify the hypothesis that the shape of the normalized distribution of retardation times  $\phi_{J^T}$  ( $\ln \tau$ ) is independent of temperature.

2. Anomalous superposition behaviour of creep compliance curves above 70°C is consistent with  $J_R^T$  increasing with temperature less rapidly than  $J_U^T$  ( $c_T > d_T > b_T$ ). Below 70°C  $c_T \simeq d_T \simeq b_T$ .

3. The activation energy  $\Delta H_\alpha$  has an approximately constant value of 21 kcal mol<sup>-1</sup> below 70°C and then increases steadily up to about 33 kcal mol<sup>-1</sup> at 120°C.

4. No evidence is found for a 60 kcal mol<sup>-1</sup> relaxation process below 40°C as observed by Miki *et al* [12].

5. The very high values of  $\Delta H_\alpha$  found by Read and Williams [6] are owing to assuming (wrongly) that the limiting moduli are independent of temperature. Estimates of  $c_T$  and  $d_T$  from the superposition results lead to corrections to these  $\Delta H_\alpha$  values that are in agreement with those of other workers.

6. A tentative explanation for  $c_T > d_T$  is that re-ordering of the crystal/amorphous interface affects  $J_R^T$  (and hence  $d_T$  and  $b_T$ ) but does not affect  $J_U^T$  (and hence  $c_T$ ).

## Acknowledgements

The author wishes to thank the Science Research Council and St John's College, Oxford for

financial support and Dr N. G. McCrum for encouragement in the course of this study.

## References

1. N. G. MCCRUM, B. E. READ and G. WILLIAMS, "Anelastic and Dielectric Effects in Polymeric Solids" (Wiley, New York, 1967).
2. Y. S. PAPIR and E. BAER, *Mater. Sci. Eng.* **8** (1971) 310.
3. H. THURN, Festschr. Carl Wurster, BASF, Ludwigshafen, 1960, p. 321.
4. Y. ISHIDA, M. MATSUO, M. ITO, M. YOSHINO, F. IRIE and M. TAKAYANAGI, *Kolloid. Z.* **174** (1961) 162.
5. N. G. MCCRUM, *J. Polymer Sci.* **54** (1961) 561.
6. B. E. READ and G. WILLIAMS, *Polymer* **2** (1961) 239.
7. M. TAKAYANAGI, *Mem. Fac. Eng., Kyushu Univ.* **13** (1963) 41.
8. K. ARISAWA, K. TSUGE and Y. WADA, *Reports Progr. Polymer Phys. Japan* **6** (1963) 151.
9. *Idem*, *Japan. J. Appl. Phys.* **4** (1965) 138.
10. M. TAKAYANAGI, K. NEKI, A. NAGAI and S. MINAMI, *Zairyo* **14** (1965) 343.
11. K. MIKI, Y. YOKOKAWA, K. HIKICHI and J. FURUICHI, *Japan. J. Appl. Phys.* **5** (1966) 818.
12. K. MIKI, K. HIKICHI and M. KANEKO, *ibid* **6** (1967) 931.
13. H. LEADERMAN, *Textile Res. J.* **11** (1941) 171; A. V. TOBOLSKY and R. D. ANDREWS, *J. Chem. Phys.* **13** (1945) 3.
14. J. D. FERRY, In "Viscoelastic Properties of Polymers" 2nd Edn. (Wiley, New York, 1970).
15. M. L. WILLIAMS, R. F. LANDEL and J. D. FERRY, *J. Amer. Chem. Soc.* **77** (1955) 3701.
16. N. G. MCCRUM and E. L. MORRIS, *Proc. Roy. Soc. London A* **281** (1964) 258.
17. E. R. FITZGERALD, L. D. GRANDINE and J. D. FERRY, *J. Appl. Phys.* **24** (1953) 650, 911.
18. Y. WADA, H. HIROSE, T. ASANO and S. FUKUTOMI, *J. Phys. Soc. Japan* **14** (1959) 1064.
19. N. G. MCCRUM, *J. Polymer Sci.* **A2** (1964) 3951.
20. K. OKANO, In "Solid State Physics", Vol. 14 (edited by F. Seitz and D. Turnbull) (Academic Press, New York, 1963).
21. C. P. BUCKLEY and N. G. MCCRUM, *J. Polymer Sci. A-2* **9** (1971) 369.
22. F. J. BALTA-CALLEJA and A. PETERLIN, *Makromol. chem.* **141** (1971) 91.
23. C. F. HAMMER, T. A. KOCH and J. F. WHITNEY, *J. Appl. Polymer Phys.* **1** (1959) 169.
24. J. MAJER and J. STEJNÝ, *Chem. Prumysl (Prague)* **12/37** (1962) 53.
25. S. TIMOSHENKO and J. N. GOODIER, In "Theory of Elasticity", 2nd edn. (Wiley, New York, 1951).
26. S. TURNER, *British Plastics*, November (1964) p. 26.
27. L. C. E. STRUIK, *Rheol. Acta* **6** (1967) 119.
28. L. C. E. STRUIK and F. R. SCHWARZL, *ibid* **8** (1969) 134.



29. K. NAGAMATSU, T. YOSHITOMI and T. TAKEMOTO, *J. Colloid Sci.* **13** (1958) 257.
30. N. G. MCCRUM and E. L. MORRIS, *Proc. Roy. Soc. London A* **292** (1966) 506.
31. A. W. THORNTON, *J. Appl. Phys.* **41** (1970) 4347.
32. W. SOMMER, *Kolloid Z.* **167** (1959) 97.
33. D. G. FESKO and N. W. TSCHOEGL, *J. Polymer Sci. C* **35** (1971) 51.
34. N. G. MCCRUM, private communication.
35. B. E. READ and G. WILLIAMS, *Trans. Faraday Soc.* **57** (1961) 1979.
36. K. TSUGE, H. ENJOJI, H. TERADA, Y. OZAWA and Y. WADA, *Japan. J. Appl. Phys.* **1** (1962) 270.
37. A. PETERLIN and E. W. FISCHER, *Z. Phys.* **159** (1960) 272.
38. K. O'LEARY and P. H. GEIL, *J. Macromol. Sci. (Phys.)* **B1** (1967) 147.
39. B. CRIST, *J. Polymer Sci. (Phys. Ed.)* **11** (1973) 635.
40. E. W. FISCHER, Y. NUKUSHIMA and Y. ITOH, *J. Polymer Sci. B* **3** (1965) 383.
41. J. D. HOFFMAN, G. WILLIAMS and E. PASSAGLIA, *J. Polymer Sci. C* **14** (1966) 173.

Received 26 June and accepted 23 July 1973.